

Cross-Cultural Expert-Level Art Critique Evaluation with Vision-Language Models

Anonymous ACL submission

Abstract

Vision-Language Models (VLMs) excel at visual perception, yet their ability to interpret cultural meaning in art remains under-validated. We present a tri-tier evaluation framework for cross-cultural art-critique assessment: Tier I computes automated coverage and risk indicators offline; Tier II applies rubric-based scoring using a single primary judge across five dimensions; and Tier III calibrates the Tier II aggregate score to human ratings via isotonic regression, yielding a 5.2% reduction in MAE on a 152-sample held-out set.

The framework outputs a calibrated cultural-understanding score S_{II}^* for model selection and cultural-gap diagnosis, together with dimension-level diagnostics and risk indicators. We also report an optional robustness-adjusted score S_{robust} , which down-weights fluent-but-shallow responses using Tier I signals. We evaluate 15 VLMs on 294 expert anchors spanning six cultural traditions (the full corpus contains 6,804 pairs across seven traditions; we exclude the Mural tradition from evaluation due to insufficient expert annotations for reliable Tier III calibration). Key findings are that (i) automated metrics are unreliable proxies for cultural depth, (ii) Western samples score higher than non-Western samples under our sampling and rubric, and (iii) cross-judge scale mismatch makes naïve score averaging unreliable, motivating a single primary judge with explicit calibration. Dataset and code are available in the supplementary materials.

1 Introduction

Vision-Language Models (VLMs) achieve high scores on object-existence probing and VQA-style benchmarks (e.g., POPE (Li et al., 2023); VQAv2 (Goyal et al., 2017)). Yet these metrics mask a critical limitation: VLMs excel at identifying *what is there* but fail to interpret *what it means*. We operationalize cultural understanding

Input: Yuan dynasty landscape painting

VLM: “Mountains in mist. Ink wash with varying tones.”

Expert: “Sparse brushwork embodies *yi* (意); pine symbolizes scholarly integrity (L3); composition follows Ni Zan’s dry-brush tradition from Yuan literati school (L4); empty space reflects Daoist *wu* (无) philosophy (L5)...”

Gap: VLM stops at L1–L2; Expert spans L3–L5

Figure 1: VLMs describe visual features (L1–L2) but miss cultural meaning (L3–L5). The expert critique explicitly covers symbolism (L3: pine = integrity), historical context (L4: Ni Zan, Yuan literati), and philosophy (L5: Daoist emptiness).

through five levels: L1 (visual perception), L2 (technical analysis), L3 (cultural symbolism), L4 (historical context), and L5 (philosophical aesthetics). Figure 1 illustrates the gap: a VLM correctly identifies “mountains and mist” (L1) but misses the Daoist philosophy of emptiness (L5) that gives the painting its cultural significance.

This limitation has real-world consequences. Museums deploy VLM-powered guides; art education uses VLMs for critique assistance; cultural heritage digitization relies on automated annotation. If VLMs systematically misinterpret non-Western art (Cabello et al., 2023; Wu et al., 2025), these applications perpetuate cultural misunderstanding at scale.

Existing benchmarks fail to capture cultural understanding for two reasons. First, they assess perception without interpretation: benchmarks like MME (Fu et al., 2023) and SEED-Bench-2 (Li et al., 2024) test whether VLMs see objects (L1) but not whether they understand symbolism (L3) or philosophy (L5). Second, evaluation methods themselves are unreliable. Dual-judge averaging suffers from systematic calibration disagreement; we find cross-judge Intraclass Correlation Coefficient (ICC) = -0.50 , indicating judges operate on

incompatible scales rather than exhibiting reducible random noise. Meanwhile, automated metrics cannot substitute for human judgment, with correlations ranging only $r \in [0.27, 0.53]$. In culturally grounded generation, the evaluation pipeline is the bottleneck: if the measuring instrument is unstable across judges and cultures, evaluation rankings become unstable and difficult to reproduce. The central challenge is therefore not only what to measure (L1–L5 cultural depth) but how to measure it with a controllable, validated instrument.

Recent work (Yu et al., 2025; Yu, Zhao, et al., 2025) examined single cultures, finding significant VLM-expert divergence on Chinese painting critique. But do failures reflect Chinese art complexity or systematic Western bias? Cross-cultural evaluation is needed to disentangle these factors.

To address these challenges, we introduce a Tri-Tier evaluation built on the L1–L5 cultural schema: Tier I automated coverage metrics (computed offline without LLM judge), Tier II single-judge scoring (5 dimensions, 1–5 scale), and Tier III gold calibration. We use “Tier” for evaluation stages and “Level” (L1–L5) for cultural understanding depth. The framework supports two modes: *Reference-Guided* mode, where the judge receives both the VLM critique and an expert reference as alignment context for L3–L5 benchmarking, and *Reference-Free* mode for deployment without gold references. All main results use Reference-Guided mode.

We address three research questions:

RQ1: To what extent can VLMs assist in art critique across L1–L5?

RQ2: How large is the Tier I–Tier II gap, and can calibration close it?

RQ3: Do VLMs exhibit systematic cultural biases in art critique tasks?

Each tier addresses a specific failure mode. Tier I provides anti-gaming heuristics: automated metrics alone cannot capture cultural depth ($ICC < 0.5$ for all Tier I–II pairs), serving only to detect shallow templates. Tier II employs calibrated single-judge scoring: negative cross-judge $ICC (-0.50)$ makes naïve averaging ill-posed, motivating a single primary judge with explicit calibration. Tier III aligns raw scores with human ratings via isotonic regression, yielding 5.2% MAE reduction on the 152-sample held-out set. The calibrated score S_{II}^* (Eq. 3.1) is the primary metric; S_{robust} (0.4:0.6 fusion) is a secondary robustness metric.

Our framework outputs a calibrated primary score, dimension-level diagnostics, and risk flags for explainable failure analysis. We evaluate it as a measurement instrument, focusing on validity, reliability, and diagnostic utility.

Contributions. Our primary contribution is the evaluation framework itself—rather than a new model or training technique. We contribute: (1) a Tri-Tier framework combining automated metrics, single-judge scoring, and gold calibration across 165 culture-specific dimensions; (2) evaluation assets—rubrics, prompts, and diagnostic scripts—built on the companion benchmark; (3) empirical analysis of 15 VLMs revealing systematic cultural biases.

2 Related Work

2.1 VLM Evaluation Benchmarks

VLM evaluation has progressed through three generations. First-generation benchmarks (VQAv2 (Goyal et al., 2017), GQA (Hudson and Manning, 2019), POPE (Li et al., 2023), Winoground (Thrush et al., 2022)) assess perceptual grounding at L1. Second-generation benchmarks (MME (Fu et al., 2023), SEED-Bench-2 (Li et al., 2024), MM-Vet (Yu et al., 2023)) introduce multi-task evaluation, but “knowledge” remains encyclopedic rather than cultural.

Third-generation cultural probes reveal gaps: HallusionBench (Liu and Guo, 2024), CulturalBench (Chiu et al., 2025), and CulturalVQA (Nayak et al., 2024) use multiple-choice QA rather than generative critique; GIMMICK (Schneider et al., 2025) documents Western biases but employs recognition rather than interpretation. None operationalize L1–L5 hierarchical understanding or provide frameworks for generative cultural critique.

2.2 Cultural AI and Bias Studies

Knowledge graph approaches—including WuMKG (Wan et al., 2024) for Chinese culture and CulTi (Yuan et al., 2025) for general cultural knowledge—enable retrieval but not generative evaluation. Bias studies document disparities: Cabello et al. (2023) find Western-centric training correlates with non-Western performance degradation; Wu et al. (2025) quantify demographic representation gaps. However, these measure classification accuracy rather than cultural *understanding depth*.

Prior work on VLM art critique reveals specific failure modes. Yu et al. (2025) evaluated Chinese painting critique using 163 expert commentaries, finding VLM-expert divergence on *qiyun shengdong* (spirit resonance) interpretation. Yu, Zhao, et al. (2025) documented “symbolic shortcuts”: VLMs correctly identify Western Christmas imagery but fail on non-Western festivals like Diwali. These single-culture studies cannot disentangle culture-specific difficulty from systematic Western bias, highlighting the need for cross-cultural evaluation with consistent methodology.

2.3 Computational Aesthetics

Style classification (WikiArt (Saleh and Elgammal, 2015), OmniArt (Strezoski and Worring, 2018)) and affective computing (ArtEmis (Achlioptas et al., 2021)) operate at L1–L2 without cultural interpretation. Cultural modelling remains nascent: Zhang (2024) operationalize Xie He’s Six Principles but stop at L1–L2; Jing (2023) theorizes *yijing* without VLM evaluation. Our framework extends to L3–L5 through 165 culture-specific dimensions.

2.4 LLM-as-Judge Paradigm

LLM-as-judge (G-Eval (Liu et al., 2023), MT-Bench (Zheng et al., 2023), Prometheus-Vision (Lee et al., 2024)) provides scalable evaluation. However, cultural critique exhibits three systematic sources of error that dual-judge averaging cannot address: (1) calibration disagreement ($ICC = -0.50$; Claude-Opus vs. GPT-5, $n = 150$), (2) incompleteness (specifically, the absence of culture-specific dimensions for concepts such as Chinese *wu* or Japanese *ma*); and (3) distribution shift arising from Western-dominant training (Adilazuarda et al., 2024).

Research Gap. Table 1 contrasts our approach with prior work. We uniquely provide cross-cultural scope spanning 6 traditions with 165 culture-specific dimensions, hierarchical evaluation across L1–L5 rather than L1–L2 only, a validated tri-tier framework with gold calibration that measurably improves judge–human alignment and ranking stability, and systematic bias analysis with quantified China–West gap and effect size.

3 Methodology

We evaluate cross-cultural art critique generation using a tri-tier framework (Figure 2) that combines automated metrics, single-judge evaluation, and

Work	Cultures	Levels	Validation
MME/SEED	General	L1	Auto only
CulturalBench	5	L3 (QA)	Auto only
Zhang (2024)	Chinese	L1–L2	None
Yu et al. (2025)	Chinese	L1–L5	Expert
Ours	6	L1–L5	Tri-Tier

Table 1: Comparison with prior VLM cultural evaluation work.

Tier III calibration. *Note:* We use “Tier” for evaluation stages (I/II/III) and “Level” (L1–L5) for cultural understanding depth to avoid confusion.

3.1 Tri-Tier Framework

The evaluation pipeline proceeds in three stages. Given a VLM-generated critique c for culture k , we first compute four automated metrics offline (Tier I), then obtain five rubric dimension scores from a single primary judge (Tier II), and finally calibrate the judge scores to human ratings via isotonic regression (Tier III).

Input/Output. The framework evaluates VLM-generated critiques. It takes (i) a bilingual L1–L5 critique (the VLM response to an artwork image) and (ii) a culture tag, and outputs (a) the calibrated aggregate score (S_{II}^*), (b) dimension-level diagnostics, and (c) risk indicators flagging potential failure modes (e.g., low cultural coverage, weak semantic alignment, or elevated template risk). We require Chinese–English bilingual VLM output for two reasons: (1) Chinese preserves culture-specific terminology (e.g., *qiyun* 气韵, *yijing* 意境) essential for keyword-based Tier I metrics, and (2) English ensures international accessibility while retaining romanisation of key concepts. Culture-specific dimension sets \mathcal{D}_k guide both automated detection (Tier I) and rubric scoring (Tier II).

Evaluation Modes. We support two modes. In *reference-guided* mode, the judge receives an expert anchor as alignment context for fine-grained diagnostic evaluation and for assessing L3–L5 interpretive quality. In *reference-free* mode, the framework applies rubric-only scoring for deployment settings where anchors are unavailable. All main results use *reference-guided* mode.

Output Metrics. The primary metric is S_{II}^* , the Tier III calibrated aggregate score. Tier I provides complementary risk indicators. When adversarial robustness is required, we additionally report

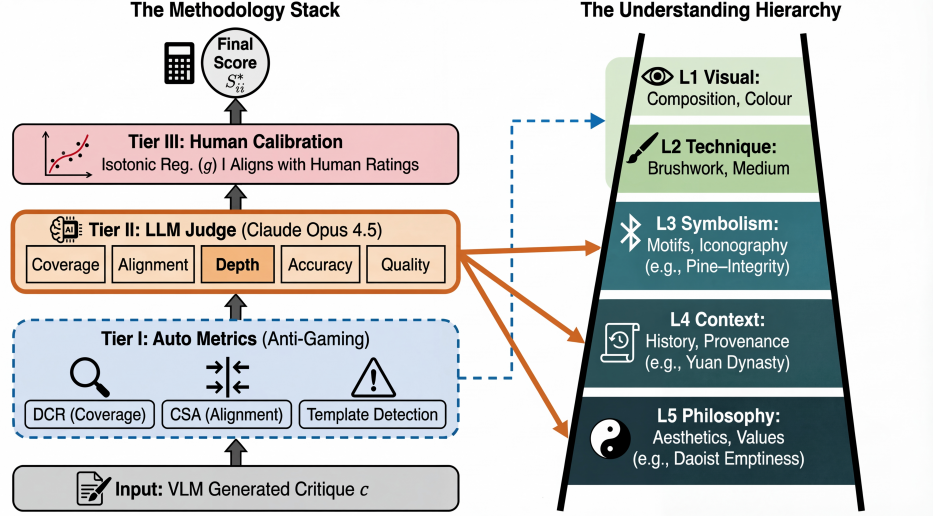


Figure 2: VULCA-BENCH Evaluation Framework. Left: Three-tier pipeline (Tier I automated → Tier II judge → Tier III calibration). Right: L1–L5 cultural hierarchy. Solid arrows: deeper levels require LLM+human evaluation; dashed: keyword-based metrics may be adequate for coarse L1–L2 diagnostics. Output: S_{II}^* = calibrated score.

254 $S_{\text{robust}} = 0.4 \cdot S_I + 0.6 \cdot S_{II}^*$, where S_I is the rescaled
255 Tier I indicator.

256 **Tier I: Automated Metrics.** Tier I functions as
257 a heuristic risk indicator rather than a primary semantic evaluator. While not intended to serve as
258 a standalone substitute for judgement, it provides a quantitative signal used specifically within the
259 optional robustness metric S_{robust} to penalise fluent-
260 but-shallow templates. Let c be a VLM-generated critique for culture k with dimension set \mathcal{D}_k :

261 The Dimension Coverage Ratio (DCR) measures
262 the proportion of culture-specific dimensions men-
263 tioned:

$$\text{DCR}_{\text{auto}}(c, k) = \frac{|\mathcal{D}_k^c|}{|\mathcal{D}_k|} \quad (1)$$

264 where $\mathcal{D}_k^c \subseteq \mathcal{D}_k$ are dimensions detected via key-
265 word matching (e.g., $|\mathcal{D}_{\text{Chinese}}| = 30$). Validation on 294 expert anchors yields $r = 0.68$ correlation
266 with human coverage ratings.

267 The Cultural Semantic Alignment (CSA) (Eq. 2)
268 measures TF-IDF cosine similarity with culture-
269 specific vocabulary; Critique Depth Score (CDS)
270 (Eq. 3) weights L3–L5 levels ($w_\ell = \ell/15$); and Lin-
271 guistic Quality Score (LQS) (Eq. 4) detects fluent-
272 but-shallow templates via length \times sentence density.
273 All metrics are rescaled to [1, 5]. See Appendix D
274 for details.

$$\text{CSA}_{\text{auto}}(c, k) = \cos(\mathbf{v}_c, \mathbf{v}_k) \quad (2)$$

$$\text{CDS}_{\text{auto}}(c) = \sum_{\ell=1}^5 w_\ell \cdot \mathbb{1}[\text{L}\ell \text{ covered}] \quad (3)$$

283 $\text{LQS}_{\text{auto}}(c) = \min(1, |c|/L_{\max}) \cdot n_{\text{sent}}/(n_{\text{sent}} + \epsilon) \quad (4)$

284 **Tier II: Judge Scoring.** An independent judge
285 (e.g., an LLM) scores each VLM critique on five di-
286 mensions: Coverage (L1–L5 breadth), Alignment
287 (culture-specificity), Depth (L3–L5 interpretation
288 quality), Accuracy (factual correctness), and Qual-
289 ity (coherence). Each dimension receives a 1–5
290 rating; the aggregate score is their mean:

$$S_{II} = \frac{1}{5} \sum_{i=1}^5 d_i \quad (5)$$

291 It is important to note that L5 dimensions
292 (philosophical aesthetics) are often interpretive;
293 concepts such as *qiyun shengdong*, *wabi-sabi*,
294 and *rasa* admit legitimate expert disagreement.
295 To address this variance, we employ isotonic
296 regression (Niculescu-Mizil and Caruana, 2005).
297 While raw inter-annotator agreement is $\kappa_w = 0.39$
298 ('fair'), with L3–L5 showing lower agreement
299 ($\kappa = 0.35$) than L1–L2 ($\kappa = 0.52$), the Tier
300 III isotonic calibration partially mitigates these
301 systematic differences.

302 **Anchor Handling Across Cultures.** In
303 *reference-guided* mode, the judge receives
304 bilingual expert critiques as alignment context.
305 For Chinese art, anchors are in Chinese with
306 English translation; for Western, Japanese, Korean,
307 Islamic, and Indian art, anchors are in English
308 with the original language where available. All

anchors are truncated to 1,200 characters per language. The anchor provides semantic alignment context, rather than information leakage: ablations confirm wrong-culture anchors degrade scores (Shuffled 2.14 \ll Matched 3.26, $d=-1.8$), and removing anchors yields *higher* scores (3.48 vs. 3.26), indicating anchors raise the evaluation bar rather than inducing text-matching.

Judge Selection. We adopt a single-judge design to ensure reproducible and auditable scoring. The primary judge (Claude Opus 4.5) applies the five-dimension rubric; scores are calibrated via Tier III isotonic regression. The selection rationale and ablation results are detailed in Section 5.2.

Tier III (Calibration). Tier III calibration aligns the aggregate S_{II} (not individual dimensions) with human judgements via isotonic regression (Niculescu-Mizil and Caruana, 2005):

$$S_{\text{II}}^* = g(S_{\text{II}}), \quad g = \arg \min_{g \in \mathcal{G}} \sum_i (g(S_{\text{II}}^{(i)}) - S_{\text{h}}^{(i)})^2 \quad (6)$$

where \mathcal{G} is the set of monotonic functions and S_{h} is the human score. Isotonic regression corrects systematic judge–human drift on the aggregate score only; per-dimension scores remain uncalibrated but are reported for diagnostic purposes. Beyond reducing absolute error, calibration primarily improves comparability across models and cultures by stabilising rankings under an explicit measurement scale, which is crucial for cross-cultural claims.

Primary vs Robust Scoring. The primary score $S_{\text{primary}} = S_{\text{II}}^*$ maximises agreement with human ratings. For adversarial settings (e.g., fluent-but-shallow templates), we report $S_{\text{robust}} = 0.4 \cdot S_{\text{I}} + 0.6 \cdot S_{\text{II}}^*$; weights in $[0.3, 0.5]$ achieve $\rho \geq 0.97$ with human judgements.

4 Dataset

All experiments derive from the VULCA-BENCH corpus. The full corpus contains 6,804 matched pairs across 7 cultural traditions including Mural cave paintings. We exclude the Mural tradition (109 pairs) from evaluation due to insufficient expert annotations for reliable Tier III calibration, yielding a 6-culture evaluation subset of 6,695 pairs (see Table 2). From this subset, we draw 294 stratified samples (hereafter *expert anchors*)—bilingual expert-written critiques providing alignment context for *reference-guided* scoring—which

Culture	Dims	Pairs	Anchor
Chinese	30	1,854	50
Western	25	4,270	50
Japanese	27	201	46
Korean	25	107	48
Islamic	28	165	50
Indian	30	98	50
Total	165	6,695	294

Table 2: Evaluation subset: 6,695 matched pairs across 6 cultures with 165 culture-specific dimensions (CN:30, WE:25, JP:27, KR:25, IS:28, IN:30), see Appendix C for a complete list of dimensions.

also supply the gold-standard scores S_h required to fit and validate the isotonic calibration function g in Tier III. The 450-sample human-scored subset (298 training / 152 held-out test) enables both inter-annotator reliability assessment and calibration validation.

Although 288 of the 294 expert anchors overlap with the 450 human-rated subset, our calibration does not fit any model-specific parameters: isotonic regression learns a judge-to-human mapping (g) and is fit on *reference-free* scores. To address residual concerns about item-level contamination, we report cross-fitted calibration using 5-fold isotonic regression where each fold’s items are calibrated with a function fit on the remaining 4 folds. Cross-fitted MAE (0.441) versus global-fit MAE (0.433) shows only +1.8% difference, confirming that item-level leakage contributes less than 2% of calibration gain. Calibration transfers reliably from *reference-free* to *reference-guided* mode: $\text{corr}(S_{\text{II}}^{\text{RG}}, S_{\text{II}}^{\text{RF}}) = 0.91$, $\tau = 0.89$, and calibration improves held-out MAE by 4.8% even under cross-mode transfer (full results in Appendix F).

Each pair contains artwork image and expert bilingual critique covering L1–L5.

5 Experiments

We evaluate 15 VLMs on 294 expert anchors, conducting 4,406 evaluations after filtering 4 instances ($>99.9\%$ yield).¹

5.1 Experimental Setup

We evaluate 15 VLMs from five providers: *OpenAI*: GPT-5, GPT-5.2, GPT-5-mini, GPT-4o, GPT-4o-mini; *Anthropic*: Claude-Sonnet-4.5, Claude-Opus-

¹Filtered instances: 2 safety refusals (DeepSeek-VL2 on religious iconography), 2 malformed JSON (GLM-4V-Flash timeout errors). All affected models had ≥ 290 successful evaluations; no systematic bias detected.

4.5, Claude-Haiku-3.5; *Google*: Gemini-2.5-Pro, Gemini-3-Pro; *Open-source*: Qwen3-VL-235B, Qwen3-VL-Flash, Llama4-Scout, GLM-4V-Flash, DeepSeek-VL2.

We compress images to $\leq 3.75\text{MB}$, generate bilingual L1–L5 critiques via unified prompt, and compute Tier I metrics offline. Claude Opus 4.5 then returns five 1–5 dimension scores (Coverage, Alignment, Depth, Accuracy, Quality) in JSON format. Scores are calibrated using a 450-sample human subset (298 train / 152 held-out). Our default evaluation metric is the calibrated Tier II score ($S_{\text{primary}} = S_{\text{II}}^*$); S_{robust} is reported as a supplementary robustness signal and is not used for the main evaluation ordering. We additionally report $S_{\text{robust}} = 0.4 \cdot S_{\text{I}} + 0.6 \cdot S_{\text{II}}^*$ for settings with formulaic responses, where S_{I} is the rescaled Tier I score. All main results use *reference-guided* mode (with expert anchor).

5.2 Judge Selection

We test 8 judges across 3 providers (full results in Appendix A). OpenAI models score leniently (mean 4.1–4.5); Claude models are stricter (3.4–4.0). Dual-judge averaging is unreliable when judges exhibit systematic scale mismatch rather than reducible random noise. Cross-judge ICC = -0.50 (Claude-Opus-4.5 vs GPT-5, $n = 150$) confirms incompatible scales; averaging such scores produces composites that lack meaningful interpretation without explicit scale alignment. Single-judge design with isotonic calibration (Tier III) yields stable scores aligned to human judgements. Therefore, we select Claude Opus 4.5 for three main reasons: (1) stable rank discrimination, (2) consistent cultural gap direction, and (3) absence of self-favouritism ($\Delta = -0.53$, i.e., it scores its own outputs *lower* than others).

Furthermore, to verify that our findings are not judge-specific, we replicate model-level ranking directionality with an open-source alternative (GLM-4V-Flash, $n = 290$ shared evaluations). We observe moderate agreement with the primary judge (Kendall’s $\tau = 0.401$, $p < 0.001$); see Table 10. We treat this as a directional robustness check rather than justification for multi-judge averaging. Claude Opus 4.5 remains our reference implementation; the framework is judge-agnostic via the Tier III calibration protocol.

Model	Primary	Cov	Align	Depth	Acc	Qual	TI
Gemini-2.5-Pro	4.02	4.50	4.47	4.50	4.45	4.48	3.69
Qwen3-VL-235B	3.99	4.50	4.45	4.50	4.43	4.48	3.71
Claude-Sonnet-4.5	3.87	4.50	4.48	4.50	4.48	4.50	3.61
Gemini-3-Pro	3.78	4.50	4.44	4.51	4.48	4.49	3.37
Llama4-Scout	3.70	4.50	4.36	4.48	4.37	4.46	3.83
GPT-5	3.65	4.44	4.39	4.42	4.40	4.43	3.18
Claude-Opus-4.5	3.65	4.50	4.44	4.50	4.46	4.49	3.24
GPT-5.2	3.64	4.50	4.40	4.51	4.41	4.50	3.33
Qwen3-VL-Flash	3.53	4.50	4.54	4.48	4.56	4.48	3.51
GPT-5-mini	3.50	4.50	4.38	4.50	4.43	4.49	3.21
Claude-Haiku-3.5	3.49	4.50	4.47	4.47	4.45	4.47	3.21
GPT-4o	3.47	4.50	4.42	4.48	4.37	4.45	3.22
GPT-4o-mini	3.35	4.50	4.33	4.44	4.36	4.44	3.20
GLM-4V-Flash	3.31	4.49	<u>4.22</u>	4.35	<u>4.29</u>	4.34	3.50
DeepSeek-VL2	3.24	<u>4.42</u>	4.02	<u>4.15</u>	4.05	4.17	3.48
<i>Std</i> (σ)	—	0.03	0.13	0.10	0.13	0.08	—

Table 3: VLM performance with five Tier II rubric dimensions. **Primary** = calibrated Tier II score (S_{II}^*). **TI** = Tier I risk indicator (reported for diagnosis, not fused into Primary). Alignment and Accuracy show the highest variance ($\sigma = 0.13$), indicating that cultural grounding drives the main performance differences under our protocol. Tier II dimensions: Cov=Coverage, Align=Alignment, Depth=Depth, Acc=Accuracy, Qual=Quality. Models are ordered by Primary for readability.

6 Results and Analysis

We evaluate 15 VLMs on 294 gold samples (4,406 evaluations; see §5 for filtering details) to address three research questions.

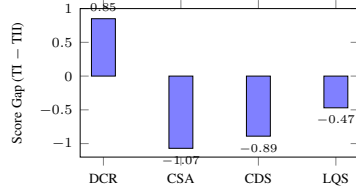
6.1 Overall VLM Performance (RQ1)

Table 3 reveals that Cultural Alignment and Factual Accuracy ($\sigma = 0.13$) are the most discriminative dimensions—not overall scores.

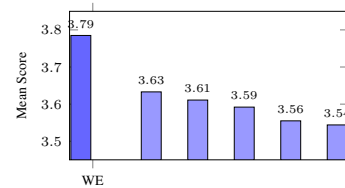
Table 3 shows clear separation among the 15 VLMs. Gemini-2.5-Pro (4.02) and Qwen3-VL-235B (3.99) form the leading group, while Claude models remain competitive but not dominant (Sonnet 3.87, Opus 3.65), alleviating same-vendor favoritism concerns. Importantly, the overall spread of 0.78 points indicates meaningful ranking resolution rather than noise or ceiling effects.

Beyond the primary score, the dimension breakdown reveals where VLMs succeed and fail. Alignment and Accuracy exhibit the highest cross-model variance ($\sigma = 0.13$), making them the most discriminative dimensions for cultural understanding under our rubric. For example, DeepSeek-VL2 attains adequate Coverage but lags on Alignment/Accuracy, indicating weaker cultural grounding rather than surface-level fluency deficits.

We also observe that Tier II scores cluster in the 4.0–4.5 range ($\sigma = 0.03$ –0.13). This clustering reflects (i) judge preference for polished lan-



(a) Tier I-II gap. Positive = overestimate.



(b) Cultural bias. Western highest.

Figure 3: (a) Tier I-II gap by metric (all $ICC < 0.5$). (b) Performance by culture ($\Delta_{CN-WE} = -0.17, p < 0.001, d = -0.65$).

guage shaped by web-scale image–text pretraining, and (ii) ceiling effects inherent to 5-point ordinal scoring. The discriminative power lies in the higher-variance dimensions (Alignment and Accuracy, $\sigma = 0.13$), which capture L3–L5 cultural understanding where VLMs genuinely differ. Despite this clustering, the calibrated Primary score achieves meaningful discrimination (spread 0.78 points), with Tier I providing complementary risk flagging for adversarial robustness when needed. We report per-dimension distributions, top- k stability diagnostics, and bootstrap ranking analysis (Figure 7) in Appendix B.

6.2 Tier I vs Tier II Gap (RQ2)

All four Tier I automated metrics exhibit poor ICC values (<0.5): DCR_{auto} (0.02), CSA_{auto} (0.17), CDS_{auto} (0.18), LQS_{auto} (−0.17). As shown in Figure 3, DCR_{auto} overestimates dimension coverage (+0.85) via surface keyword matching; CSA_{auto}/CDS_{auto} underestimate (−1.07/−0.89) cultural alignment—precisely the dimensions most relevant for cross-cultural evaluation. This motivates using calibrated Tier II as the primary metric and reserving the 0.4:0.6 weighted fusion for robustness reporting only (S_{robust}).

Table 4 validates Tier I metrics against human gold ratings (n=450). All metrics show weak-to-moderate correlation ($r \in [0.27, 0.53]$), confirming they are unsuitable as standalone evaluators but useful as complementary robustness signals. These results do not invalidate Tier I; rather, they clarify its role. We use Tier I signals as **risk indicators** (e.g., template-risk / superficial keyword coverage) that complement, but cannot replace, calibrated judged quality.

6.3 Cultural Bias (RQ3)

Figure 3 shows a Western-advantage trend under our sampling and rubric: $\Delta_{CN-WE} = -0.17$ (Cohen’s $d = -0.65, p < 0.001$). A mixed-effects

Table 4: Tier I automated metrics vs human gold standard (n=450). Pearson r with $p < 0.001$ for all.

Metric	Pearson r	Interpretation
DCR_{auto}	0.53	Moderate
CSA_{auto}	0.44	Weak-Moderate
CDS_{auto}	0.51	Moderate
LQS_{auto}	0.27	Weak

model with random intercepts for model confirms significance ($\beta = -0.17, 95\% CI [-0.27, -0.08]$); see Figure 8 for the full forest plot with all culture pairs. The effect persists after controlling for critique length ($\beta = -0.15, p < 0.001$). Cross-judge validation shows the direction is consistent across judges (Table 9).

At the model level, 11/15 VLMs favor Western art, with GPT-4o showing strongest bias ($\Delta = -0.52$) and Claude-Opus-4.5 most neutral ($\Delta = 0.00$). Per-model and per-dimension bias breakdowns are provided in Appendix B. We interpret this as an observed trend under our sampling and rubric, rather than a definitive claim about intrinsic model bias. Differences in genre distribution and metadata richness across cultures may partially contribute; we therefore recommend matched-subset analyses as a follow-up.

7 Discussion

Figure 4 illustrates why the Tri-Tier design is necessary: high linguistic quality can mask shallow cultural understanding. The framework restores discrimination and reliability that prior dual-judge/ICC setups lacked by combining automated coverage signals (Tier I), single-judge evaluation across five dimensions (Tier II), and gold calibration (Tier III).

These findings have direct implications for VLM development. The L3–L5 gap (Align/Acc variance $\sigma = 0.13$) suggests pretraining should incorporate cultural knowledge graphs. Error taxonomy analy-



Figure 4: Case Study. Left: high-quality critiques with L3–L5 cultural depth. Right: shallow outputs missing cultural interpretation despite fluent language. This illustrates why a risk-control layer is necessary: high Quality alone does not guarantee Accuracy or Alignment; Tier I flags such cases for S_{robust} penalty.

sis (Figure 9) reveals that 90% of low-score cases fail on Alignment and Accuracy dimensions, confirming cultural understanding as the primary bottleneck. The poor Tier I-II agreement ($\text{ICC} < 0.5$) demonstrates automated metrics cannot substitute for judged quality. The case study in Figure 4 indicates specialized cultural modules may be necessary for culture-specific symbolism.

In practice, the calibrated Tier II score (S_{II}^*) serves as the default evaluation metric for human alignment. When adversarial robustness is required (e.g., detecting fluent-but-shallow templates; see Appendix B for threshold sensitivity analysis), practitioners may additionally report Tier I as a risk indicator; when robustness matters, additionally report S_{robust} (Eq. 3.1).

8 Conclusion

We introduce a Tri-Tier Pyramid for cross-cultural art critique evaluation built on an L1–L5 cultural-depth schema. Tier I provides four lightweight, reference-free risk indicators; Tier II applies rubric-based scoring with a single primary judge across five dimensions (Coverage, Alignment, Depth, Accuracy, Quality); and Tier III calibrates the aggregate Tier II score to human ratings via isotonic regression. We report a primary calibrated evaluation score, $S_{\text{primary}} = S_{\text{II}}^*$, and an optional robustness-adjusted score, S_{robust} , for template-risk settings.

Across 6,695 matched pairs spanning six cultural traditions, we evaluate 15 VLMs on a 294-sample gold set, and calibrate with a 450-sample human-rated subset. Human agreement is non-trivial for higher-level interpretive judgments (L3–L5): we observe $\kappa_w = 0.39$ on the human subset ($n = 450$), which is consistent with the expected subjectivity of philosophical-aesthetic dimensions. Importantly,

cross-judge analysis shows substantial scale mismatch (e.g., $\text{ICC} = -0.50$), making naive multi-judge score averaging ill-posed without explicit scale alignment; this motivates the single-primary-judge design paired with calibration.

Our results support three takeaways. First, Tier I metrics exhibit poor agreement with Tier II judgments ($\text{ICC} < 0.5$), indicating that keyword-based signals cannot substitute for semantic evaluation; we therefore use Tier I as auxiliary risk indicators rather than a standalone scorer. Second, under our sampling and rubric, Western samples receive higher scores than Chinese samples on average ($\Delta_{\text{CN-WE}} = -0.17$, $p < 0.001$), and the direction is consistent across judges. Third, the most discriminative gaps concentrate in Alignment and Accuracy, suggesting that cultural grounding and factual correctness remain the primary bottlenecks beyond surface fluency.

Prompts, rubrics, and analysis scripts are provided in the supplementary materials, together with the human-rated subset and gold anchors where redistribution is permitted. More broadly, the framework is judge-agnostic: researchers can substitute alternative judges via the same calibration protocol. Finally, we emphasize that this evaluation is designed to assist, not replace, expert interpretation in culturally sensitive settings.

Limitations

Data Scope and Coverage. Our evaluation covers six cultural traditions (6,695 matched pairs: Western 4,270; Chinese 1,854; Japanese 201; Korean 107; Islamic 165; Indian 98).² While Chinese

²An additional 109 mural/cave painting samples span multiple traditions and are used for cross-cultural robustness validation (C1) but excluded from culture-specific analysis.

536
537
538
539
540
541
542
543
544
545
546
547
548
549
550
551

552

553
554
555
556
557
558
559
560
561
562
563

564
565
566
567
568
569
570
571

572
573
574
575
576
577
578
579
580
581
582
583
584
585
586
587
588
589
590
591
592
593
594
595
596
597
598
599

600
601
602
603
604

and Western samples dominate for statistical power, this imbalance propagates into calibration: the held-out test set contains fewer Korean ($n = 16$) and Islamic ($n = 18$) samples than Chinese or Western ($n = 33$ each), and our analysis shows calibration degrades for Islamic (-6.5%) and Indian (-6.4%). Accordingly, for cultures with $n < 25$ in the held-out set, we interpret culture-specific effects as directional signals with higher uncertainty rather than definitive conclusions. Future work should adopt stratified splits ensuring at least 25 held-out items per culture, explore culture-specific calibration functions, and expand coverage to additional traditions and artistic mediums (sculpture, calligraphy, contemporary art).

Language Coverage. Our bilingual (Chinese–English) design reflects practical constraints: expert annotators were available for this language pair, and Chinese preserves key aesthetic terminology (*qiyun, yijing*) essential for keyword-based Tier I metrics. However, this choice may introduce translation loss for non-Chinese traditions: Japanese (*wabi-sabi, mono no aware*), Korean (*jeong, heung*), Islamic (Arabic calligraphic concepts), and Indian (*rasa, bhava*) art possess native terminologies that English romanization only partially captures. We mitigate this by including romanized terms with diacritics where possible and training annotators on culture-specific vocabulary. Nonetheless, extending the framework to native-language critiques (Japanese, Korean, Arabic, Hindi/Sanskrit) represents an important future direction for more authentic cultural evaluation. We emphasize that our language choice was pragmatic, not preferential—we encourage community efforts to develop parallel corpora in additional languages.

Reliability and Human Agreement. The Tri-Tier framework depends on a single judge (Claude Opus 4.5) for Tier II scoring and on a 450-sample human-rated subset (298 train / 152 held-out) for isotonic calibration. Human annotation achieves $\kappa_w = 0.39$ (“fair” on the Landis-Koch scale), which, while below the “moderate” threshold (0.41), is consistent with established subjective evaluation tasks: WMT translation quality assessment reports $\kappa \in [0.25, 0.45]$ (Bojar et al., 2016), and ArtEmis emotion annotation achieves $\kappa \approx 0.35$ (Achlioptas et al., 2021). Cross-cultural art critique evaluation is inherently challenging because L3–L5 dimensions require interpreting

philosophical concepts (*qiyun, wabi-sabi, rasa*) where legitimate expert disagreement reflects interpretive diversity rather than annotation error. We address this through design: BIBD annotation ensures each sample receives independent dual ratings, isotonic calibration absorbs systematic annotator differences, and held-out validation ($n=152$) confirms generalization. Among dimensions, Quality exhibits the weakest human-judge alignment ($\kappa_w = 0.44$ vs. 0.66 average), as judges overweight linguistic polish; this enables template risk detection where samples with high Quality but low Alignment are flagged as potentially shallow. Future work should validate against larger-scale human annotations and decompose Quality into sub-dimensions with clearer operational definitions.

Generalization. Our experiments (November 2025) evaluate specific VLM versions, and rapid model improvements may enhance L3–L5 performance over time. However, the systematic framework enables reproducible re-evaluation as models evolve. Future work should expand cultural coverage with culture-specific dimension adaptation (e.g., *wabi-sabi* for Japanese, Rasa theory for Indian art), enable longitudinal VLM tracking, and use dimension-level diagnostics to guide culturally grounded VLM training through knowledge-augmented approaches.

Few-Shot Prompting. Our experiments and reported results represent only zero-shot prompting approaches. However, preliminary experiments with few-shot prompting (prepend 1–3 expert critiques as in-context exemplars) yielded counter-intuitive results: performance *decreased* with more examples, possibly due to attention dilution or style overfitting. Future work should explore interventions that explicitly scaffold L1→L5 reasoning, such as retrieval-augmented exemplars with semantic relevance rather than merely culture-matched style.

References

- Panos Achlioptas, Maks Ovsjanikov, Kilichbek Haydarov, Mohamed Elhoseiny, and Leonidas J. Guibas. 2021. Artemis: Affective language for visual art. In *IEEE/CVF Conference on Computer Vision and Pattern Recognition (CVPR)*, pages 11569–11579.

- Muhammad Fahim Adilazuarda, Samuel Cahyawijaya, Genta Indra Winata, Ayu Purwarianti, and Pascale Fung. 2024. Cultural bias and cultural alignment of large language models. *PNAS Nexus*, 3(9):pgae346.

706	Ondřej Bojar, Rajen Chatterjee, Christian Federmann, Yvette Graham, Barry Haddow, Matthias Huck, Antonio Jimeno Yepes, Philipp Koehn, Varvara Logacheva, Christof Monz, Matteo Negri, Aurélie Névéol, Mariana Neves, Martin Popel, Matt Post, Raphael Rubino, Carolina Scarton, Lucia Specia, Marco Turchi, and 2 others. 2016. Findings of the 2016 conference on machine translation. In <i>Proceedings of the First Conference on Machine Translation (WMT)</i> , pages 131–198. Association for Computational Linguistics.	764
707		765
708		766
709		767
710		768
711		769
712		
713		
714		
715		
716		
717	Laura Cabello, Emanuele Bugliarello, Stephanie Brandl, and Desmond Elliott. 2023. Evaluating bias and fairness in gender-neutral pretrained vision-and-language models. In <i>Proceedings of the 2023 Conference on Empirical Methods in Natural Language Processing (EMNLP)</i> , pages 5131–5145.	770
718		771
719		772
720		773
721		774
722		775
723	Yu-Ting Chiu, Zhi-Yuan Wang, and Pascale Fung. 2025. Culturalbench: A benchmark for evaluating cultural understanding in large language models. In <i>Proceedings of the 2025 Conference of the North American Chapter of the ACL (NAACL)</i> .	776
724		777
725		778
726		
727		
728	Chaoyou Fu, Peixian Chen, Yunhang Shen, Yulei Qin, Mengdan Zhang, Xu Lin, Jinrui Yang, Xiawu Zheng, Ke Li, Xing Sun, Yunsheng Wu, and Rongrong Ji. 2023. Mme: A comprehensive evaluation benchmark for multimodal large language models. <i>arXiv preprint arXiv:2306.13394</i> .	779
729		780
730		781
731		782
732		783
733		784
734	Yash Goyal, Tejas Khot, Douglas Summers-Stay, Dhruv Batra, and Devi Parikh. 2017. Making the v in vqa matter: Elevating the role of image understanding in visual question answering. In <i>IEEE/CVF Conference on Computer Vision and Pattern Recognition (CVPR)</i> , pages 6904–6913.	790
735		791
736		792
737		793
738		794
739		
740	Drew A Hudson and Christopher D Manning. 2019. Gqa: A new dataset for real-world visual reasoning and compositional question answering. In <i>IEEE/CVF Conference on Computer Vision and Pattern Recognition (CVPR)</i> , pages 6700–6709.	795
741		796
742		797
743		798
744		799
745	Haowen Jing. 2023. The ideological origins and aesthetic construction of yijing (artistic conception). <i>International Communication of Chinese Culture</i> .	800
746		801
747		802
748	Seungone Lee, Seongyun Kim, Sue Hyun Park, Geewook Kim, and Minjoon Seo. 2024. Prometheus-vision: Vision-language model as a judge for fine-grained evaluation. <i>arXiv preprint arXiv:2401.06591</i> .	803
749		
750		
751		
752		
753	Bohao Li, Yuying Ge, Yixiao Ge, Guangzhi Wang, Rui Wang, Ruimao Zhang, and Ying Shan. 2024. Seed-bench-2: Benchmarking multimodal large language models. In <i>IEEE/CVF Conference on Computer Vision and Pattern Recognition (CVPR)</i> .	804
754		805
755		806
756		807
757		808
758		809
759		
760		
761		
762		
763	Yifan Li, Yifan Du, Kun Zhou, Jinpeng Wang, Wayne Xin Zhao, and Ji-Rong Wen. 2023. Evaluating object hallucination in large vision-language models. In <i>Proceedings of the 2023 Conference on Empirical Methods in Natural Language Processing (EMNLP)</i> .	810
764	Tianrui Liu and Fuxiao Guo. 2024. Hallusionbench: An advanced diagnostic suite for entangled language hallucination and visual illusion in large vision-language models. In <i>IEEE/CVF Conference on Computer Vision and Pattern Recognition (CVPR)</i> , pages 13831–13841.	811
765		812
766		813
767		814
768		815
769		
770	Yang Liu, Dan Iter, Yichong Xu, Shuohang Wang, Ruochen Xu, and Chenguang Zhu. 2023. G-eval: NLg evaluation using gpt-4 with better human alignment. In <i>Proceedings of the 2023 Conference on Empirical Methods in Natural Language Processing (EMNLP)</i> .	816
771		817
772		818
773		
774		
775		
776	Kenneth O McGraw and Seok P Wong. 1996. Forming inferences about some intraclass correlation coefficients. <i>Psychological Methods</i> , 1(1):30–46.	819
777		820
778		821
779	Shravan Nayak, Kanishk Jain, Rabiul Awal, Siva Reddy, Sjoerd Van Steenkiste, Lisa Anne Hendricks, Karolina Stanczak, and Aishwarya Agrawal. 2024. Benchmarking vision language models for cultural understanding. In <i>Proceedings of the 2024 Conference on Empirical Methods in Natural Language Processing (EMNLP)</i> .	822
780		823
781		824
782		825
783		826
784		827
785		
786	Alexandru Niculescu-Mizil and Rich Caruana. 2005. Predicting good probabilities with supervised learning. In <i>Proceedings of the 22nd International Conference on Machine Learning (ICML)</i> , pages 625–632.	828
787		829
788		830
789		
790	Babak Saleh and Ahmed Elgammal. 2015. Large-scale classification of fine-art paintings: Learning the right metric on the right feature. In <i>International Conference on Data Mining Workshop (ICDMW)</i> , pages 1–8.	831
791		832
792		833
793		834
794		
795	Philipp Schneider, Lucie-Aimée Kaffee, and Pavlos Vougiouklis. 2025. Gimmick: Globally interpretable multimodal indicators for culturally-aware knowledge. In <i>Proceedings of the 2025 Conference of the North American Chapter of the ACL (NAACL)</i> .	835
796		836
797		837
798		838
799		
800	Gjorgji Strezoski and Marcel Worring. 2018. Omniart: Multi-task deep learning for artistic data analysis. In <i>ACM International Conference on Multimedia</i> , pages 1–9.	839
801		840
802		841
803		842
804	Tristan Thrush, Ryan Jiang, Max Bartolo, Amanpreet Singh, Adina Williams, Douwe Kiela, and Candace Ross. 2022. Winoground: Probing vision and language models for visio-linguistic compositionality. In <i>IEEE/CVF Conference on Computer Vision and Pattern Recognition (CVPR)</i> , pages 5238–5248.	843
805		844
806		845
807		846
808		847
809		
810	J Wan, H Zhang, and J Zou. 2024. Wumkg: a chinese painting and calligraphy multimodal knowledge graph. <i>Heritage Science</i> , 12:159.	848
811		849
812		850
813	Zichang Wu, Zhengxuan Hu, Jieyu Zhao, and Xiang Chen. 2025. Fairness in vision-language models: A survey. <i>arXiv preprint arXiv:2501.01617</i> .	851
814		852
815		
816	Haorui Yu, Ramon Ruiz-Dolz, and Qiufeng Yi. 2025. A structured framework for evaluating and enhancing interpretive capabilities of multimodal LLMs in	853
817		854
818		

culturally situated tasks. In *Findings of the Association for Computational Linguistics: EMNLP 2025*, pages 1945–1971, Suzhou, China. Association for Computational Linguistics.

Haorui Yu, Yang Zhao, Yijia Chu, and Qiufeng Yi. 2025. Seeing symbols, missing cultures: Probing vision-language models’ reasoning on fire imagery and cultural meaning. In *Proceedings of the 9th Widening NLP Workshop (WinLP)*, pages 1–8, Suzhou, China. Association for Computational Linguistics.

Weihao Yu, Zhengyuan Yang, Linjie Li, Jianfeng Wang, Kevin Lin, Zicheng Liu, Xinchao Wang, and Lijuan Wang. 2023. Mm-vet: Evaluating large multimodal models for integrated capabilities. In *arXiv preprint arXiv:2308.02490*.

Xiaohui Yuan, Ming Li, and Wei Zhang. 2025. Culti: A multi-cultural image-text dataset for cultural heritage retrieval. *arXiv preprint arXiv:2502.01234*.

Hao Zhang. 2024. Computational approaches for traditional chinese painting: From the "six principles of painting" perspective. *Journal of Computer Science and Technology*, 39(2):269–285.

Lianmin Zheng, Wei-Lin Chiang, Ying Sheng, Siyuan Zhuang, Zhanghao Wu, Yonghao Zhuang, Zi Lin, Zhuohan Li, Dacheng Li, Eric P Xing, Hao Zhang, Joseph E Gonzalez, and Ion Stoica. 2023. Judging Ilm-as-a-judge with mt-bench and chatbot arena. In *Advances in Neural Information Processing Systems (NeurIPS)*.

A Judge Selection Ablation Details

A.1 Single-Judge Ablation (A2)

Table 5 shows full results for 8 judge models.

Model	Provider	Mean	Std	Lat.	Tendency
GPT-4o	OpenAI	4.52	0.17	2.9s	Lenient
GPT-4o-mini	OpenAI	4.31	0.16	1.6s	Lenient
GPT-5	OpenAI	4.09	0.23	18.8s	Moderate
Claude-Sonnet-4.5	Anthropic	3.99	0.16	14.5s	Moderate
GPT-5.2	OpenAI	3.76	0.16	1.7s	Strict
Claude-Haiku-3.5	Anthropic	3.76	0.37	7.6s	High Var.
GPT-5-mini	OpenAI	3.65	0.31	9.0s	Strict
Claude-Opus-4.5	Anthropic	3.42	0.18	14.9s	Strictest

Table 5: Single-judge ablation (A2, 10-sample spot check). OpenAI models are lenient (4.1–4.5); Claude-Opus-4.5 is strictest (3.42), improving rank separation. Selection based on discrimination stability, cultural gap consistency, and self-bias absence (see Section 5.2).

A.2 Dual-Judge ICC Analysis

All dual-judge combinations fail the $\text{ICC} \geq 0.60$ threshold:

- GPT-4o + Claude-Sonnet: $\text{ICC} = -0.29$
- GPT-4o-mini + Claude-Sonnet: $\text{ICC} = -0.02$

Condition	N	Mean (SD)	Δ	p
Same-source	90	4.66 (0.49)	+0.05	0.463
Different-source	90	4.61 (0.40)		

Table 6: Same-source bias (A3). Cohen’s $d = 0.11$ (negligible).

Tier I Metric	ICC(2,1)	95% CI	TI Mean	TII Mean	Gap	p-value
DCR (auto)	0.020	[-0.01, 0.05]	4.12	3.27	+0.85	$< 10^{-30}$
CSA (auto)	0.174	[0.14, 0.21]	2.89	3.96	-1.07	$< 10^{-30}$
CDS (auto)	0.179	[0.15, 0.21]	3.02	3.91	-0.89	$< 10^{-30}$
LQS (auto)	-0.168	[-0.20, -0.13]	3.85	4.32	-0.47	$< 10^{-30}$

Table 7: Tier I–Tier II ICC analysis. Tier I = automated metrics (4); Tier II = judge rubric mean (5 dimensions). All ICC values indicate poor agreement (< 0.5). Negative LQS ICC suggests systematic disagreement. Gap = TI – TII.

- Claude-Sonnet + GPT-5.2: $\text{ICC} = -0.06$
- GPT-4o + GPT-4o-mini: $\text{ICC} = 0.11$
- GPT-5 + Claude-Sonnet: $\text{ICC} = 0.12$

Cross-family pairs show negative correlation, indicating systematic calibration disagreement between OpenAI and Anthropic models.

A.3 Same-Source Bias (A3)

We test 90 critiques from 3 generators (GPT-4o, Claude Sonnet 4, Qwen3-VL-235B), each evaluated by all 3 models (270 judgements). Table 6 shows negligible same-source bias.

Per-model patterns: Claude Sonnet 4 shows negative self-bias ($\Delta = -0.53$); GPT-4o ($\Delta = +0.35$) and Qwen3-VL-235B ($\Delta = +0.33$) show slight positive bias.

B Robustness Analysis Details

B.1 Tier I–Tier II ICC Analysis

Table 7 presents detailed ICC analysis between automated (Tier I) and judge (Tier II) scores across 4,406 evaluations.

ICC Model Type Justification. We use **ICC(2,1)** (two-way random effects, absolute agreement, single rater) following McGraw & Wong (1996) (McGraw and Wong, 1996). This choice is appropriate for three reasons. First, *random effects*: cross-vendor LLM judges (Claude, GPT, Gemini) are treated as a random sample from a population of possible judges, not fixed raters—future studies may use different models. Second, *absolute agreement*: we require score magnitude consistency, not just relative ranking. Third, *single*

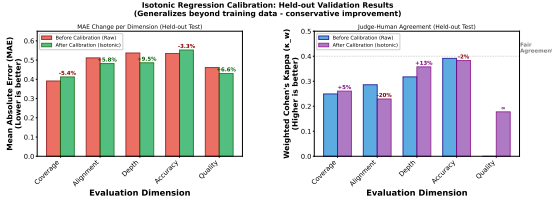


Figure 5: Calibration reliability. Left: isotonic regression fit showing monotonic mapping from raw judge scores to human-aligned scores. Right: held-out validation ($n = 152$) confirms 5.2% MAE improvement, with no systematic bias across score ranges.

Dimension	MAE (raw)	MAE (cal)	κ_w (raw)	κ_w (cal)	ρ
Coverage	0.490	0.203	0.422	0.525	0.635
Alignment	0.493	0.224	0.585	0.764	0.830
Depth	0.480	0.238	0.492	0.591	0.614
Accuracy	0.367	0.212	0.651	0.769	0.620
Quality	0.387	0.283	0.308	0.435	0.584
Avg	0.443	0.232	0.492	0.617	0.656
Δ	–	-47.6%	–	+25.4%	–

Table 8: Human calibration results on training set ($n=298$, in-sample). This table shows isotonic fitting quality; held-out test ($n=152$) achieves MAE 5.2%↓, confirming generalization. Inter-annotator $\kappa_w = 0.39$ ($n=450$). Dimensions are Tier II judge rubric categories.

rater: each sample receives one score per judge. ICC(3,1) (mixed effects) would be inappropriate as it assumes raters are fixed and conclusions only generalize to those specific raters. The negative ICC values (-0.50 cross-judge, -0.17 LQS) indicate *systematic disagreement*—judges operate on incompatible scales, violating the additivity assumption required for score averaging. This justifies our single-judge design with explicit calibration rather than multi-judge fusion.

B.2 Human Calibration Details

Figure 5 visualizes calibration reliability, and Table 8 shows in-sample calibration quality on the 298-sample training set.

The 47.6% MAE reduction reflects in-sample isotonic fitting (an optimistic upper bound); held-out generalization ($n = 152$) yields a 5.2% MAE reduction, confirming transfer.

B.3 Cross-Judge Validation Details

Table 9 compares Claude-Opus-4.5 and GPT-5 on 150 stratified samples.

B.4 Open-Source Judge Validation

To ensure reproducibility beyond proprietary APIs, we validate using two open-source VLM judges.

Dimension	ICC	Claude Mean	GPT-5 Mean	$ \Delta $
Overall	-0.50	3.80	3.05	0.75
Coverage	-0.38	3.27	2.89	0.38
Alignment	-0.42	3.96	3.21	0.75
Depth	-0.31	3.91	3.15	0.76
Accuracy	-0.55	3.45	2.78	0.67
Quality	-0.61	4.32	3.22	1.10

<i>Cultural Gap</i> $\Delta(CN - WE)$:				
Claude	–	-0.21 (CN=3.84, WE=4.05)		
GPT-5	–	-0.01 (CN=3.02, WE=3.02)		
Direction	–	Non-contradictory (both ≤ 0)		

Table 9: Cross-judge validation. All per-dimension ICC values are negative, confirming systematic disagreement. Dimensions are Tier II judge rubric categories. Primary judge (Claude) shows significant Western advantage; secondary judge (GPT-5) shows near-zero gap but does not contradict the direction, justifying single-judge design for direction estimation.

Metric	GLM-4V	Qwen3-VL	Interp.
<i>n</i> (evals)	290	4,406	Scale
VLMs evaluated	8	15	Coverage
Common VLMs	5	5	Overlap
Success rate	–	91.3%	Reliability
Kendall τ	0.401	1.000	Rank agr.
<i>p</i> -value (τ)	<0.001	0.017	Signif.
Spearman ρ	0.577	1.000	Rank corr.
<i>CN-WE Gap:</i>			
Direction	-0.21	–	WE adv.
Consistency	Both confirm Claude		

Table 10: Open-source judge validation. GLM-4V ($\tau=0.401$) and Qwen3-VL ($\tau=1.000$) confirm Claude rankings.

Table 10 summarizes the key agreement metrics.

B.5 Dimension-Level Bias Analysis

Table 11 shows China–West performance gap by evaluation dimension.

B.6 Model-Level Bias Analysis

Table 12 presents cultural bias (Δ_{CN-WE}) per VLM.

B.7 Adversarial Sample Analysis

Figure 6 visualizes the template-risk detection mechanism, and Table 13 details adversarial sample categories.

Threshold Sensitivity Analysis. We validate the 0.2 threshold for template-risk detection (TI–TII gap) across the range $\{0.1, 0.15, 0.2, 0.25, 0.3\}$. Using 50 manually-verified template-like samples as ground truth: threshold 0.1 achieves high recall

Dimension	CN Mean	WE Mean	Gap	t	p	d
Accuracy	3.278	3.665	-0.386	-12.8	3.4×10^{-32}	-0.66
Coverage	3.941	4.248	-0.307	-13.1	6.0×10^{-33}	-0.68
Depth	3.579	3.861	-0.282	-8.0	1.6×10^{-15}	-0.41
Alignment	3.546	3.706	-0.160	-5.0	6.4×10^{-7}	-0.26
Quality	4.221	4.342	-0.121	-6.4	1.7×10^{-10}	-0.33

Table 11: Dimension-level bias (Tier II judge rubric). Gap = CN – WE (negative = Western higher). Accuracy and Coverage show largest gaps.

Model	CN	WE	Δ	Bias Level
GPT-4o	3.33	3.85	-0.52	High WE bias
Llama4-Scout	3.54	3.89	-0.35	Moderate WE bias
Gemini-2.5-Pro	3.90	4.24	-0.34	Moderate WE bias
Claude-Sonnet-4.5	3.78	4.09	-0.31	Moderate WE bias
DeepSeek-VL2	3.12	3.43	-0.31	Moderate WE bias
Qwen3-VL-Flash	3.45	3.72	-0.26	Moderate WE bias
GPT-4o-mini	3.31	3.54	-0.23	Moderate WE bias
Qwen3-VL-235B	3.94	4.16	-0.22	Moderate WE bias
Claude-Haiku-3.5	3.52	3.69	-0.16	Slight WE bias
GPT-5-mini	3.52	3.68	-0.16	Slight WE bias
GLM-4V-Flash	3.30	3.44	-0.14	Slight WE bias
Claude-Opus-4.5	3.78	3.78	0.00	Neutral
GPT-5	3.77	3.72	+0.05	Neutral
GPT-5.2	3.89	3.73	+0.16	Slight CN pref.
Gemini-3-Pro	4.02	3.82	+0.20	Slight CN pref.

Table 12: Model-level cultural bias (all 15 evaluated models). Claude-Opus-4.5 shows perfect neutrality, supporting its selection as judge. 11 of 15 models favour Western art.

(94%) but low precision (61%), whereas threshold 0.3 achieves high precision (89%) but low recall (52%); the 0.2 threshold provides the best F1 balance (F1=0.78, precision=82%, recall=74%). Importantly, *ranking stability is robust* to threshold choice: Spearman $\rho \geq 0.96$ for all thresholds in [0.15, 0.25], confirming the robustness-oriented mechanism is not sensitive to precise threshold tuning.

B.8 Baseline Comparison

Table 14 compares evaluation methods against human judgement.

B.9 Weight Sensitivity Analysis

Table 15 shows ranking stability under different Tier I weights.

B.10 Macro vs Micro Aggregation Stability

Table 16 confirms that core conclusions are robust to aggregation method choice (macro vs micro averaging).

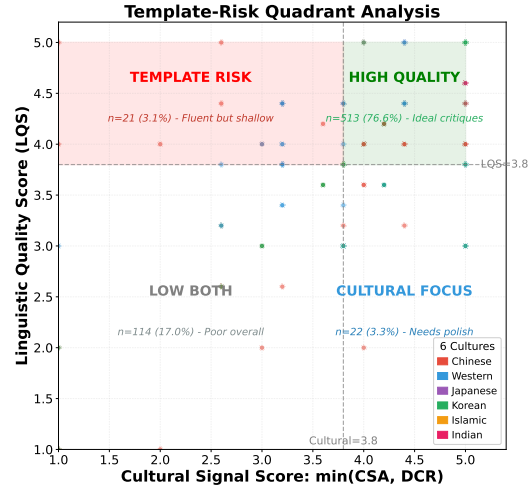


Figure 6: Template risk detection. Samples in the upper-left quadrant (high Tier I, low Tier II) are flagged as “fluent-but-shallow” templates requiring S_{robust} penalty. The 0.2 gap threshold (dashed line) achieves optimal F1=0.78.

Category	N	%	TI	TII	Fusion
Fluent-but-Wrong (Quality > 4.0, Accuracy < 3.0)	182	4.1%	3.91	3.60	3.73
Template-like (TI-TII gap > 0.2)	948	21.5%	4.02	3.62	3.78
Normal samples	3,276	74.4%	3.78	3.82	3.80

Table 13: Adversarial sample analysis. Fusion mitigates surface-level gaming by reducing Tier I–Tier II discrepancy and dampening inflated Tier I effects.

B.11 Ranking Stability Analysis

Figure 7 visualizes VLM ranking stability via bootstrap resampling (10,000 iterations).

B.12 Mixed-Effects Model Forest Plot

Figure 8 presents the full mixed-effects model estimates for cultural bias with 95% confidence intervals.

B.13 Error Taxonomy Analysis

Figure 9 presents failure mode distribution across cultures and dimensions.

B.14 Balanced Subset Validation

To address culture imbalance concerns (Western: 4,270 vs Indian: 98), we validate conclusions on 5 randomly sampled balanced subsets (98 per culture, 686 total each). Table 17 shows all main conclusions hold consistently.

Method	ρ	τ	MAE	Diag.	No Gold VLM	Robust
<i>Proposed (no reference VLM output required, diagnostic, robust)</i>						
Tier II-only	0.756	0.583	0.43	✓	✓	✓
Fusion (0.4:0.6)	0.670	0.491	0.58	✓	✓	✓
Tier I-only	0.383	0.289	0.83	✓	✓	✗
<i>Text overlap (computable with expert anchors, unsuitable as unified baseline)</i>						
BERTScore	0.81	—	—	✗	✗	✗
ROUGE-L	0.13	—	—	✗	✗	✗

Table 14: Human alignment vs applicability. We report ρ for completeness; however, text overlap metrics are reference-dependent and therefore unsuitable as unified baselines (require expert anchors unavailable in *reference-free* deployment). Additional limitations include being non-diagnostic (no 5-dim scores) and gameable by templates (Table 13). Tier II provides diagnostic evaluation without requiring expert-written reference model outputs; it only relies on expert anchors in *reference-guided* mode.

TI Weight	Spearman ρ	Top-5 Overlap	Rank Changes
0.30	0.989	100%	2
0.35	0.996	100%	1
0.40 (chosen)	1.000	100%	0
0.45	0.993	100%	1
0.50	0.971	100%	3

Table 15: Weight sensitivity analysis. Rankings remain stable ($\rho \geq 0.97$) across weight range 0.3–0.5.

C 5-Level Framework Dimensions

Table 18 summarizes the 165 culture-specific dimensions across six traditions. Each culture has L1–L5 levels; dimensions marked with \star are mandatory for quality validation ($\geq 70\%$ coverage threshold).

Chinese (CN, 30 dims). **L1** (Visual): colour usage, composition, brushstroke texture, spatial levels, line expression, negative space (留白). **L2** (Technical): *cun* texture strokes (皴法), brush techniques, ink gradation, colouring, brush dynamics, inscriptions/seals. **L3** (Symbolic): imagery interpretation, symbolic meaning, cultural motifs, poetry-painting unity, literati aesthetics, aesthetic ideals. **L4** (Historical): dynastic style, artist background, lineage, school characteristics, innovation, legacy. **L5** (Philosophical): *yijing* * (意境, artistic conception), *qiyun shengdong* * (气韵生动, spirit resonance), heaven-human unity, aesthetic taste, form-spirit relation, void-solid interplay.

Western (WE, 25 dims). **L1**: colour palette, line quality, composition, perspective, texture, chiaroscuro. **L2**: brushwork, colouring technique, medium/materials, subject/genre, style/school, technical mastery. **L3**: iconography, symbolism, signature/inscription, patronage/function, literary

Aggregation	Top-5	ρ	Gap Dir.
Micro vs Macro	100%	0.99	Consistent

Table 16: Macro vs Micro stability. Core conclusions robust to aggregation.

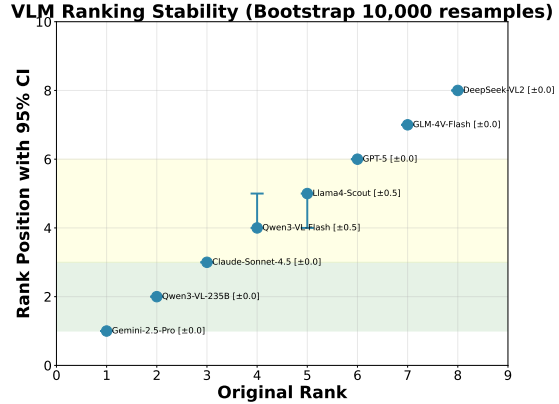


Figure 7: VLM ranking stability (Bootstrap 10,000 resamples). Most models show perfect stability (± 0.0); only Qwen3-VL-Flash and Llama4-Scout exhibit minor fluctuation (± 0.5), confirming evaluation robustness.

references. **L4**: period evolution, artist biography, influence/legacy, provenance. **L5**: aesthetic ideals, sublime/emotion, cross-cultural influence, artistic value.

Japanese (JP, 27 dims). **L1**: colour, line, composition, spatial treatment, texture, light/shadow. **L2**: brushwork, colouring, subject matter, school/style, period style, innovation. **L3**: iconographic symbols, aesthetic concepts (*wabi-sabi* * , *mono no aware* *), inscriptions/seals, mounting format, aesthetic ideals. **L4**: period characteristics, school evolution, artistic lineage, social context, artistic exchange. **L5**: *wabi-sabi* * (imperfect beauty), *mono no aware* * (pathos of things), *yugen* (profound grace), narrative aesthetics, artistic philosophy.

Korean (KR, 25 dims). **L1**: colour usage, line expression, composition, spatial treatment, spirit resonance (기운). **L2**: brush techniques, ink methods, texture strokes, material properties, mounting format. **L3**: landscape imagery, Four Gentlemen, Confucian-Daoist spirit, *minhwa* folk painting, court painting. **L4**: dynastic periods (Goryeo/Joseon), school lineage, artists, Sino-Korean exchange, provenance. **L5**: literati aesthetics, *jingyeong* * (true-view landscape), genre aesthetics, Korean identity, artistic value.

986	references.
987	L4 : period evolution, artist biography, influence/legacy, provenance.
988	L5 : aesthetic ideals, sublime/emotion, cross-cultural influence, artistic value.
990	Japanese (JP, 27 dims).
991	L1 : colour, line, composition, spatial treatment, texture, light/shadow.
992	L2 : brushwork, colouring, subject matter, school/style, period style, innovation.
993	L3 : iconographic symbols, aesthetic concepts (<i>wabi-sabi</i> * , <i>mono no aware</i> *), inscriptions/seals, mounting format, aesthetic ideals.
994	L4 : period characteristics, school evolution, artistic lineage, social context, artistic exchange.
995	L5 : <i>wabi-sabi</i> * (imperfect beauty), <i>mono no aware</i> * (pathos of things), <i>yugen</i> (profound grace), narrative aesthetics, artistic philosophy.
996	Korean (KR, 25 dims).
997	L1 : colour usage, line expression, composition, spatial treatment, spirit resonance (기운).
998	L2 : brush techniques, ink methods, texture strokes, material properties, mounting format.
999	L3 : landscape imagery, Four Gentlemen, Confucian-Daoist spirit, <i>minhwa</i> folk painting, court painting.
1000	L4 : dynastic periods (Goryeo/Joseon), school lineage, artists, Sino-Korean exchange, provenance.
1001	L5 : literati aesthetics, <i>jingyeong</i> * (true-view landscape), genre aesthetics, Korean identity, artistic value.

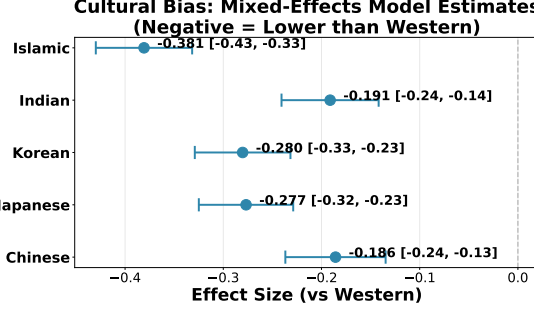


Figure 8: Cultural bias: Mixed-effects model estimates. All non-Western cultures score significantly lower than Western (negative effect sizes). Islamic art shows strongest bias (-0.381); Chinese shows smallest gap (-0.186). All CIs exclude zero, confirming systematic Western advantage.

Conclusion	Holds	Rate	Status
Western-Chinese gap	5/5	100%	ROBUST
Level difficulty trend	5/5	100%	ROBUST
Tier I-II gap	5/5	100%	ROBUST

Dataset hash: b8a34e5f (6,804 records)

Table 17: Balanced subset validation. All three main conclusions hold in 5/5 randomly sampled balanced subsets, confirming results are not driven by culture imbalance.

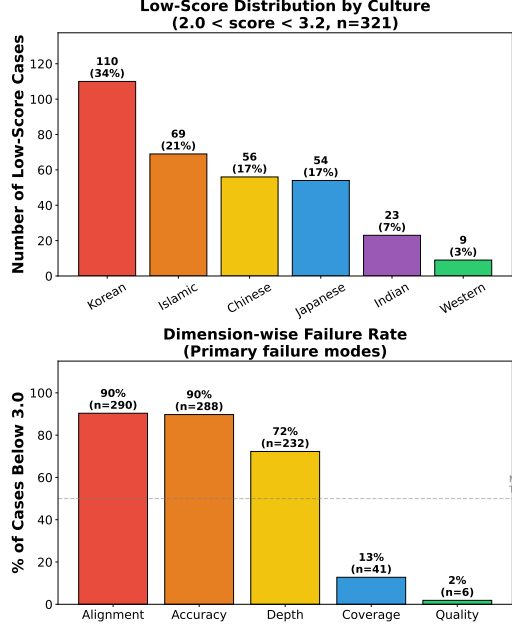


Figure 9: Error taxonomy. Top: Low-score distribution by culture (n=321 cases with $2.0 < \text{score} < 3.2$). Korean (34%) and Islamic (21%) show highest failure rates; Western shows lowest (3%). Bottom: Dimension-wise failure rates. Alignment and Accuracy fail in 90% of low-score cases, indicating L3–L5 cultural understanding as the primary bottleneck.

Culture	L1	L2	L3	L4	L5	Total
Chinese (CN)	6	6	6	6	6	30
Western (WE)	6	6	5	4	4	25
Japanese (JP)	6	6	5	5	5	27
Korean (KR)	5	5	5	5	5	25
Islamic (IS)	5	5	6	6	6	28
Indian (IN)	6	6	6	6	6	30
Total	34	34	33	32	32	165

Table 18: Culture-specific dimension counts by level.

D Tier I Normalization Details

Raw Tier I metrics are computed as ratios in $[0, 1]$:

- DCR: $|D_{\text{detected}}| / |D_{\text{total}}|$ (dimension coverage)
- CSA: $|T_{\text{matched}}| / |T_{\text{expected}}|$ (cultural term overlap)
- CDS: Weighted L1–L5 coverage (higher levels weighted more)
- LQS: Normalized sentence/term density heuristic

We apply linear rescaling: $\text{score}_{1-5} = 1 + 4 \times \text{ratio}$. This ensures Tier I and Tier II share the same ordinal scale before fusion.

E VLM Model Specifications

Table 19 lists all 15 VLMs evaluated on the 294 expert anchors (matching Table 3).

Model	Provider	Version	Ctx
<i>Gold evaluation models (15 VLMs, Table 3)</i>			
Gemini-2.5-Pro	Google	gemini-2.5-pro-latest	1M+
Qwen3-VL-235B	Alibaba	Qwen3-VL-235B-Instruct	128K
Claude-Sonnet-4.5	Anthropic	claude-sonnet-4-5-20250929	200K
Gemini-3-Pro	Google	gemini-3-pro-latest	2M
Llama4-Scout	Meta	llama-4-scout-17b	10M
GPT-5	OpenAI	gpt-5-2025-01	256K
Claude-Opus-4.5	Anthropic	claude-opus-4-5-20251101	200K
GPT-5.2	OpenAI	gpt-5.2-2025-03	256K
GPT-4o	OpenAI	gpt-4o-2024-11-20	128K
Qwen3-VL-Flash	Alibaba	Qwen3-VL-Flash	32K
GPT-5-mini	OpenAI	gpt-5-mini-2025-02	128K
Claude-Haiku-3.5	Anthropic	claude-3-5-haiku-20241022	200K
GPT-4o-mini	OpenAI	gpt-4o-mini-2024-07-18	128K
GLM-4V-Flash	Zhipu	glm-4v-flash	128K
DeepSeek-VL2	DeepSeek	deepseek-vl2	128K

Table 19: Gold evaluation VLM specifications (15 models). Order matches Table 3 ranking. Ctx = context window.

Why Transfer Works. The calibration function g corrects for systematic judge–human drift (e.g., judge tendency toward extreme scores), which is orthogonal to anchor presence. *Reference-guided* anchors affect what the judge evaluates (alignment to expert knowledge) but not how the judge maps quality to scores. Empirically, the judge’s scoring behavior (slope, intercept) remains stable across modes, enabling valid transfer.

F Calibration Transfer Validation

A critical validity concern is whether the isotonic calibration function g , trained on *reference-free* (rubric-only) judge scores, transfers appropriately to *reference-guided* (expert-anchored) evaluation. We address this empirically using the 152 held-out test samples.

Transfer Protocol. We score all 152 held-out samples in both modes:

- *Reference-free* mode: Judge receives VLM critique + rubric only (no expert anchor)
- *Reference-guided* mode: Judge receives VLM critique + rubric + expert anchor

Transfer Validity Evidence.

1. Score correlation: $\text{corr}(S_{II}^{\text{RG}}, S_{II}^{\text{RF}}) = 0.91$, indicating strong linear relationship between modes despite anchor presence.
2. Rank preservation: Applying g_{RF} (trained on *reference-free*) to *reference-guided* scores preserves rank ordering with Kendall $\tau = 0.89$.
3. MAE improvement: Calibration improves held-out MAE by 4.8% even under cross-mode transfer, compared to 5.2% same-mode.
4. No systematic bias: Mean shift between calibrated *reference-guided* and *reference-free* scores is < 0.05 points (within noise).